Snatcher: A Highly Mobile Chameleon-Inspired Shooting and Rapidly Retracting Manipulator

Dong-Jun Lee and Gwang-Pil Jung

***Abstract*—Chameleon tongue-like manipulators have the potential to be quite useful for mobile systems to overcome access issues by allowing them to reach distant targets in an instant. For example, a quadrotor with this manipulator will be able to snatch distant targets instead of hovering and picking up. In this letter, we present a chameleon-inspired shooting and rapidly retracting manipulator, which is lightweight, compact, and ultimately suitable for mobile systems. To make this possible, two design strategies are proposed: to use a wind-up spring as an energy source and to employ an active clutch to selectively distribute the energy. The wind-up spring enables the device to keep supplying the stored energy for a long time, compared to normal torsion springs. The active clutch controls the direction and the timing of the energy supply, which allows to deploy and retract the end-effector. Thanks to these design strategies, the device achieves snatching manipulation while maintaining compact and lightweight. In result, the Snatcher has a size of 120 $\times$ 85 $\times$ 85 mm, weighs 117.48 g, and brings a 30 g mass located at 0.8 m away within 600 ms.**

***Index Terms*—Biologically-inspired robots, shooting manipulator, chameleon-inspired robotic arm.**

I. Introduction

CHAMELEONS have the ability to manipulate distant targets positioned over 1.5 body length away. Furthermore, the launching speed is over 3.5 m/s and the acceleration reaches up to 500 m/s^2 [1]–[3]. Thanks to the surprisingly fast speed, the chameleons can bring the distant targets back to their mouth within a second. If this amazing manipulation method is applied to the mobile systems, it has the potential to diversify the applicable areas by providing the concept of fast snatching.

For example, the chameleon-inspired manipulator could be an option for small-scale unmanned aerial vehicles (UAV) such as quadrotors. Currently, the UAVs employ conventional robotic arms to manipulate objects [4]–[7] by following two steps: approaching closely and picking up. For simple tasks, such as going straight and bringing an object, there exists room for reducing time and energy consumption during the process. If there is a compact, lightweight, and rapidly operating manipulator like a chameleon's tongue, it would be helpful for the UAVs to efficiently manipulate distant targets.

There already have been chameleon tongue-like manipulators as shown in Table I. Debray firstly proposed a chameleon-inspired manipulator using a DC motor and a coil gun [8]. The coil gun accelerates the magnet connected to the DC motor's pulley. After the ejection of the magnet, the DC motor winds the string to retract the magnet. Hatakeyama *et al.* implemented a chameleon-like shooting manipulator based on the air compressor and a solenoid valve [9], [10]. By using the impulse force from the compressor, the manipulator finishes touching the 0.7 m distant target within 250 ms. The retraction was done by the string connected to the elastic cantilever. Mochiyama *et al.* also employed an air compressor and a solenoid valve to achieve 10 m reaching [11]. Kaneko *et al.* proposed a capturing robot that finishes the gripping of a falling ball in 25 ms [12]. A DC motor and an electromagnet are used to store and release the energy. To adjust the capturing point, an additional DC motor is employed. These manipulators have shown successful shooting and retracting performance. In terms of usability, however, there exists a portability issue coming from heavy and bulky actuation systems required to generate the impulse force.

The whole actuation system needs to be compact and lightweight to apply the chameleon-like manipulator to small-scale quadrotors. We especially consider quadrotors similar to the M200 V2 from DJI, which have the maximum payload capacity of 1.45 kg. Compact actuation systems that can generate impact force are easily seen in milli-scale jumping robots. The miniature jumping robots converts the actuator's energy into elastic materials and release the stored energy in an instant, which is the process of power amplification. By doing so, the robots generate high force while maintaining fast speed.

To generate the impact force, jumping robots have employed a variety of energy storage and release mechanisms. Most of the milli-scale jumping robots have used parallel elastic actuation [13]–[21]. They use high gear ratio motors and linkages to get a large mechanical reduction. Accordingly, they easily stretch the elastic components connected in parallel. Another approach is to employ a series elastic actuation method [22], [23]. The actuator deforms the connected elastic component in series and the component operates the jumping linkage to utilize the mechanical advantage. Existing jumping robots have successfully achieved high power actuation. To directly apply those methods, however, is not easy due to the following reasons:

- Our system requires an actuator that has long displacement output rather than a high impact force. Most of the jumping robots, however, focus on high impact force with a short displacement output.

Manuscript received January 31, 2020; accepted June 22, 2020. Date of publication July 21, 2020; date of current version August 4, 2020. This letter was recommended for publication by Associate Editor Micky Rakotondrabe and Editor Xinyu Liu upon evaluation of the Reviewers' comments. This work was supported in part by the Korean Government (MSIT) under Grants NRF-2016R1A5A1938472, NRF-2019R1F1A1063356, and in part by (MOTIE)(KIAT-P0008473, HRD Program for Industrial Innovation). *(Corresponding author: Gwang-Pil Jung.)*

The authors are with the Department of Mechanical and Automotive Engineering, SeoulTech, Seoul 01811, South Korea (e-mail: pzwu1024@gmail.com; gpjung@seoultech.ac.kr).

This letter has supplementary downloadable material available at https://ieeexplore.ieee.org, provided by the authors.

Digital Object Identifier 10.1109/LRA.2020.3010744

TABLE I
CHAMELEON TONGUE-INSPIRED MANIPULATORS

	Verified retracting distance, mass, time	Shooting mechanism	Retracting mechanism	Portability
Debray et al. [8]	0.3m, 1.0g mass, ~250ms	Coil gun	DC motor or elastomer	Challenging due to the power supply
Hatakeyama et al. [9, 10]	0.7m, falling 0.3g mass, ~270ms	Compressed air, solenoid valve	Elastic cantilever or Passive inertial wheel	Challenging due to air compressor -
Mochiyama et al. [11]	10m, no retracting mass, focused on shooting	Compressed air	-	Challenging due to air compressor
Makoto et al. [12]	0.16m, small ball (mass is unknown) ,25ms for capturing only	Stored energy in linear spring	Wire winding using DC motor	Challenging due to actuators and transmissions (arm and grippers alone weigh 100g)
This work	0.8m, 30g, 594ms 0.80m, 0g, 480ms	Pre-stored energy in wind-up spring	Pre-stored energy in wind-up spring	Possible, Size 120x85x85 (mm), 117.48g

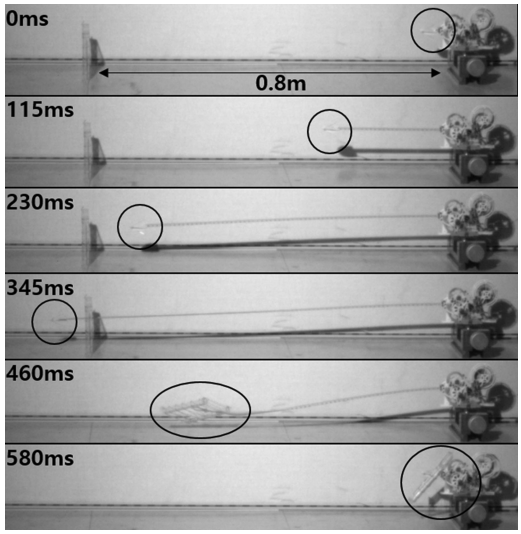

Fig. 1. A highly mobile shooting and rapidly retracting manipulator. The manipulator is snatching a 30 g mass 0.8 m away within 600 ms.

- The direction of energy flow needs to be actively controlled to launch and rapidly retract the manipulator.
- Linkages for the mechanical lever effect need to be minimized to make a compact actuation system.

To satisfy the above requirements, in this letter, we suggest a novel actuation system for the highly mobile chameleon-inspired shooting and rapidly retracting manipulator, called Snatcher. Key design strategies are an employment of a wind-up spring (also called a mainspring) and an active clutch. The wind-up spring enables the Snatcher to utilize the long displacement output compared to normal torsional springs. An active clutch allows not only to control the direction of the energy flow but also to adjust the supply timing of the energy. By applying these strategies, the chameleon-inspired manipulator, the Snatcher, is successfully made as shown in Fig. 1. The Snatcher has a size of $120 \times 85 \times 85$ mm, weighs 117.48 g, and brings a 30 g mass located at 0.8 m away within 600 ms.

The paper is organized as follows: The design section explains the working principles of the Snatcher and describes the structure of the whole actuation system. The modeling section analyzes the output torque of the actuator and the dynamics are taken into consideration to find optimal design parameters. In the experiment section, launching and retracting tests are done to verify the manipulator's performance.

II. DESIGN

In this section, biological inspiration, conceptual design, and working principles are stated. Biological inspiration explains how chameleon's tongue has evolved and how the tongue works.

The manipulator is described by dividing into four parts – the tapeline to function as a deployable robotic arm, geared feeders to wind and unwind the tapeline, a series elastic actuator to store the elastic energy, and an active clutch to control the energy flow.

A. Chameleon's Tongue

Chameleons have evolved from the Lepidosauria to Squamata, and finally to Iguania which contains snakes, lizards, chameleons [24]. Unlike other Iguanians, chameleons prefer to eat hymenopterans that are active and flying [25]. The different things between chameleons and other Iguanians are telescopic eyes, Zygodactyly, ballistic tongue, prehensile tail. Especially, the ballistic tongue makes it useful to catch active and distant prey in an instant [25].

The chameleon's tongue mechanism is made up of various tissues, muscles, and bones [1], [26]. The components of this structure work complexly to accelerate the tongue in an instant in the desired direction, adhering target to the tip of the tongue and bringing it back [1]. A hyoid and accelerator muscles protrude the tongue. After reaching prey, a hyoglossus muscle retracts the tongue [2].

Instead of using the hyoid muscle for accelerating the tongue, the Snatcher employs an elastic component and stores the energy to launch the end-effector. For the retraction, chameleons activate the hyoglossus muscle while the Snatcher changes the direction of the energy flow by using an active clutch.

B. Deployable Robotic Arm

The basic purpose of the chameleon-inspired manipulator is to reach distant targets. Therefore, we need a long robotic arm to achieve distant manipulation. For portability, however, the manipulator has to become compact when it is not in use. Moreover, for practical use, the manipulator needs to maintain relatively high stiffness when fully deployed. To fulfill these requirements, a steel tapeline has been chosen as the robotic arm. In Fig. 2(a), the steel tapeline is wrapped around the spool.

As shown in Fig. 2(a), there are two geared feeders and the tapeline passes between the feeders. That is, the steel tapeline is wound and unwound using geared feeders. For the successful manipulation, therefore, the no-slip condition between the

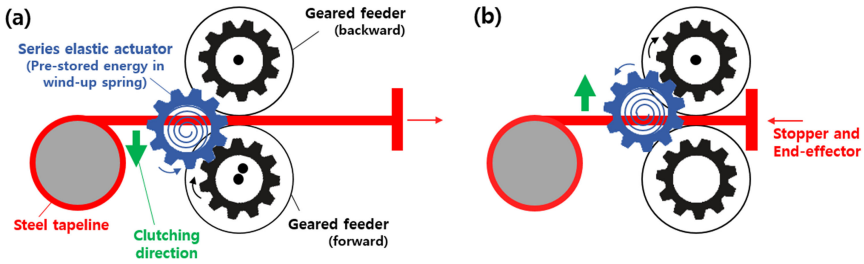

Fig. 2. Schematic of the chameleon-inspired manipulator. (a) Forward manipulation and (b) backward manipulation. The SEA rotates in a single direction where the pre-stored energy is released. Where and when to provide the pre-stored energy is determined by the active clutch.

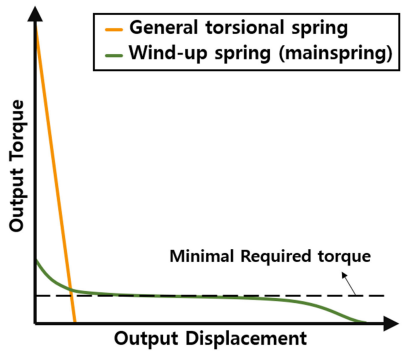

Fig. 3. Torque curves of two springs. Wind-up springs have extremely long displacement output compared to general torsional springs.

tapeline and the geared feeders should be guaranteed by providing enough friction. The friction is determined based on the normal force, F_N, and the friction coefficient, μ, between the feeder and the tapeline. If the external force, F_{ext} shown in Fig. 9, exceeds the friction force, μF_N, the slippage starts to occur. As a result, the device fails in shooting and retraction. To provide enough friction and to assure no-slip condition, we decided to increase both the friction coefficient and the normal force. To this end, polymer (dragon skin, Smooth-On) straps with the thickness of 2 mm are fabricated and applied to the circumference of the feeders.

C. Series Elastic Actuation

The proposed manipulator uses the tapeline as a robotic arm. The geared feeders are employed to wind and unwind the tapeline. To deploy and retract the tapeline up to 0.8 m using the geared feeders, then the feeders are required to rotate about 6 revolutions (2160 degrees). Considering that normal torsional springs have an angular displacement of less than one revolution, we determine to use a wind-up spring as energy storage. Wind-up springs normally have more than 4000 degrees of the angular displacement, which is at least 10 times longer than that of torsion springs.

Fig. 3 shows the output torque and the displacement of a torsion spring and a wind-up spring. They show substantially different torque curves although both springs have the same amount of stored energy. The torsion spring case has high peak torque at the beginning and the torque stiffly drops to zero. In the case of the wind-up spring, it has relatively low torque but shows a long flatter central section. So, if the torque of the flatter central section is higher than the minimally required torque of our system, we can make the best use of the output displacement while satisfying the torque requirement. The long flatter central section also enables the series elastic actuator (SEA) to generate similar torque output without controlling parameters only if the wind-up spring is kept charged.

Detail design of the SEA is shown in Fig. 4. One end of wind-up spring is directly connected to the SEA motor's axis through the arbor. The other end is connected to the barrel. The barrel has gear at its circumference and transfers the stored energy to the geared feeders.

Fig. 5 shows how the SEA motor works and the wind-up spring is charged. The SEA motor stores energy until the wind-up spring is fully charged. The amount of stored energy in the wind-up spring is estimated based on data from two encoders. In Fig. 4, one is located at the SEA motor and the other is installed to the deploying feeder. By calculating the difference between the two encoders, the deformation of the wind-up spring and accordingly the amount of the stored energy are estimated in real-time. In Fig. 5. the SEA motor keeps rotating before the difference reaches the 12 revolutions, which means the full charge of the wind-up spring.

D. Active Clutch

The key to this manipulator is how to distribute the energy stored in a single source. Depending on where and when to provide energy, the system shows substantially different aspects. To control this energy flow, an active clutch is employed.

The active clutch determines the position of the series elastic actuator and the connected barrel's gear as shown in Fig. 2. The barrel's gear transmits the pre-stored energy in the wind-up spring located inside the barrel. When the barrel's gear contacts the geared feeder at the bottom, the tapeline is deployed following the rotating direction of the feeder. If the active clutch moves the SEA to the geared feeder at the top, the rotating direction suddenly changes in the opposite direction. Therefore, the deployed tapeline starts to be retracted until the stopper meets the mainframe.

Detail design of the active clutch is shown in Fig. 4. A miniature servo motor has been employed to control the position of the SEA as shown in Fig. 4(b) and (c). Depending on the operating direction of the servo motor, the barrel's gear contacts one of the geared feeders. To reduce the clutching delay, besides, the distance between the barrel's gear and the feeders' gear is tightly adjusted. In Fig. 2, the barrel's gear always contacts at least one feeder's gear. As soon as the barrel's

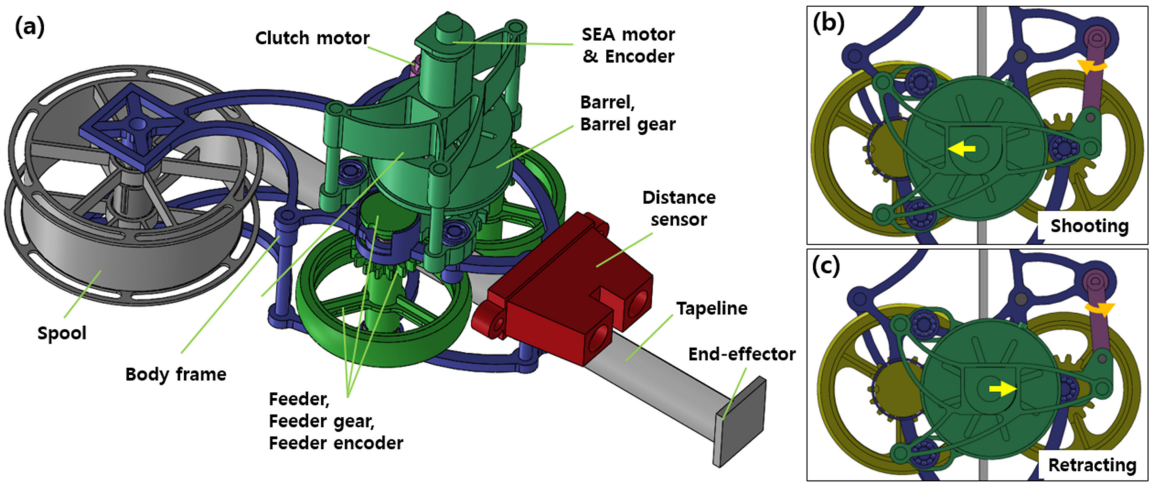

Fig. 4. Detail design of the manipulation system. (a) Whole system. (b) and (c) show how to clutch.

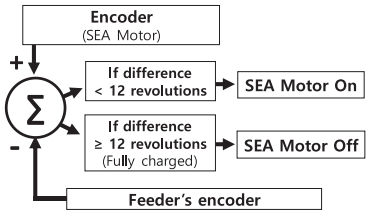

Fig. 5. SEA motor working process. The SEA motor rotates until the wind-up spring is fully charged. Even when the energy is being released, the SEA motor still works.

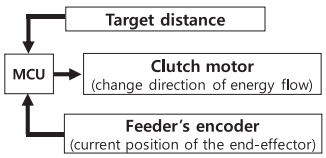

Fig. 6. Target distance control process.

gear detaches from this gear, the barrel's gear instantly touches the other feeder's gear.

E. Target Distance Control

The active clutch controls the direction of energy flow and this deploys or retracts the tapeline. To precisely reach a distant target object, to control the timing for changing the direction of the energy flow is important. To make this possible, a simple block diagram of the distance control is given in Fig. 6. The target distance is given to the MCU. The current position of the end-effector is calculated based on a magnetic encoder installed to the geared feeder. Since there hardly exists slippage between the feeders and the tapeline, the position of the end-effector can be precisely estimated in real-time. Based on the information from the given target distance and the encoder data, the clutch motor moves the SEA to change the direction of the energy flow.

F. Other Components

The overall block diagram of the controller board is shown in Fig. 7. The actuation system employs a lightweight control board

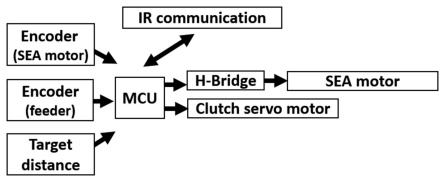

Fig. 7. Block diagram of the controller board.

TABLE II
MASS BUDGET

Components	Quantity (ea.)	Mass (g)	Mass ratio (%)
Body frame	1	10.46	8.90
Forward geared feeder	1	5.40	4.60
Backward geared feeder	1	5.23	4.46
DC motor (encoder included)	1	10.05	8.55
Clutch servo motor	1	3.93	3.35
Barrel	1	11.60	9.88
Wind-up spring	1	13.30	11.32
Feeder encoder & magnet	1	1.41	1.20
Tapeline	1	35.93	30.58
Lipo battery	1	8.57	7.29
Distance sensor	1	5.55	4.72
Controller board	1	6.05	5.15
Total	-	117.48	100.0

(Teensy 3.2, PJRC) and uses IR communication. The SEA motor and the servo motor (hs5305-hd, HiTec Inc.) are controlled by the H-bridge (DF robot, Inc.) and the PWM signal, respectively. The SEA motor uses 150:1 geared DC motor with an embedded Hall effect encoder (Pololu Inc.) and the encoder has a resolution of 0.2 degrees. The other magnetic encoder (Hall effect encoder, i2A systems Inc.) installed to the feeder has a resolution of 0.25 degrees. An IR-based distance sensor (GP2Y0A02YK0F, Sharp Inc.) is employed to determine the target distance. The whole mass budget of the system is given in Table II.

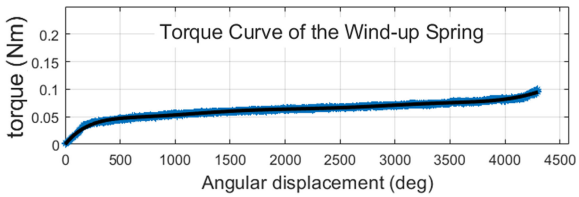

Fig. 8. Torque data and the fitted curve of the wind-up spring.

TABLE III
COEFFICIENTS OF THE POLYNOMIAL

a_o	a_1	a_2	a_3
0.0642	0.2440	-5.1654x10^{-4}	5.9330x10^{-7}
a_4	a_5	a_6	a_7
-3.8491x10^{-10}	1.4543x10^{-13}	-3.1586x10^{-17}	3.6364x10^{-21}
a_8	-	-	-
-1.7074 x10^{-25}	-	-	-

III. ANALYSIS

A. Wind-up Spring Analysis

The proposed manipulator has employed a wind-up spring to utilize the long angular displacement output. Therefore, to investigate the properties of the wind-up spring is important to understand the actuation system. To this end, we measure the torque by varying the angular displacement.

Fig. 8 shows the torque curve of the wind-up spring. As we predicted, the wind-up spring has long angular displacement as 12 revolutions which are about 4300 degrees. Also, the central flatter region is shown. The range of the region is about 4000 degrees and the torque output does not deviate much from 65 mNm. This means that the wind-up spring generates a torque of similar magnitude, even while the wind-up spring is released by 11 revolutions.

The relation between the torque and the angular displacement is non-linear and therefore it is hard to define unique spring constant. To solve this problem, curve fitting has been done using 8$^{\text{th}}$ order polynomial as shown in Fig. 8 and the torque equation is given as follows:

$$T_s = \sum_{i=0}^{i=8} a_i \theta^i \tag{1}$$

where T_s is the torque of the wind-up spring, θ is the angular displacement, and the coefficients are given in Table III.

B. Dynamics

The stored energy in the wind-up spring is transferred to the barrel, the feeder, and lastly the tapeline. At every stage, there exists mechanical reduction and this affects the performance of the manipulator. To find the appropriate gear ratio for the fastest shooting and retracting, the dynamics of the manipulator has been considered. Fig. 9 indicates the simplified model and the parameters. The equations of motion for the barrel, the feeder, and the end-effector are given as Eq. (2), Eq. (5), and Eq. (6), respectively.

$$\sum \tau_b = -T_{b,s} + f_{b,fg} r_b = I_b \ddot{\theta}_b \tag{2}$$

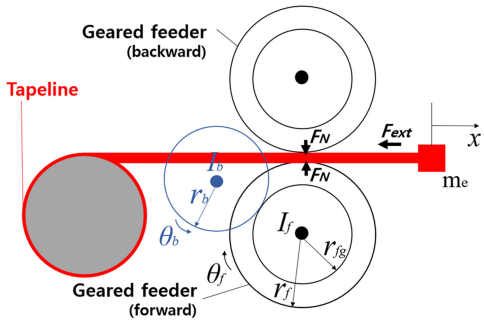

Fig. 9. Modeling parameters.

where $T_{b,s}$ is the torque acting on the barrel by the wind-up spring, I_b and θ_b are the rotational inertia and the angular displacement of the barrel, respectively.

The torque, $T_{b,s}$, is given as follows based on the torque curve of the wind-up spring.

$$T_{b,s} = \sum_{i=0}^{i=8} a_i {\theta_b}^i \tag{3}$$

The toques exerting on the feeder is given as follows:

$$\sum \tau_f = -f_{fg,\ b} r_{fg} + f_{f,e} r_f = I_f \ddot{\theta}_f \tag{4}$$

$$\ddot{\theta}_f = \frac{r_b}{r_{fg}} \ddot{\theta}_b \ (\text{gear ratio}, r_b/r_f) \tag{5}$$

where $f_{fg,b}$ is the force acting on the feeder's gear, r_{fg} is the radius of the feeder's gear, I_f is the rotational inertia of the feeder, θ_f is the angular displacement of the feeder.

$$\sum f_e = f_{e,\ f} - sgn\left(f_{e,\ f}\right) f_{e,\ t} = m_e \ddot{x} \tag{6}$$

$$\ddot{x} = r_f \ddot{\theta}_f = r_f \frac{r_b}{r_{fg}} \ddot{\theta}_b \quad (\text{no} - \text{slip condition}) \tag{7}$$

where $f_{e,f}$ is the force acting on the end-effector, x is the displacement of the end-effector, $f_{e,t}$ is the force from the inner torsion spring of the tapeline.

The above equations are numerically simulated using the ODE45 function in MATLAB. The initial conditions are given as $\theta_b(0) = 4300°$, $\dot{\theta}_b(0) = 0$.

IV. RESULTS

In this section, parametric studies using the dynamic model are done to decide the size of the feeder and the feeder's gear. By varying the radii of them, the required time and the required revolutions for 0.8 m manipulation are investigated.

To test the performance of the Snatcher, manipulation time, and the target distance accuracy are examined by varying the position of the target. Also, the Snatcher is applied to a mobile system to show the possibility to be used for real-world applications.

A. Simulated Results

Fig. 10 shows the simulated results of a 0.8 m manipulation based on dynamic modeling. Fig. 10(a) indicates the position of the end-effector depending on the time. The end-effector

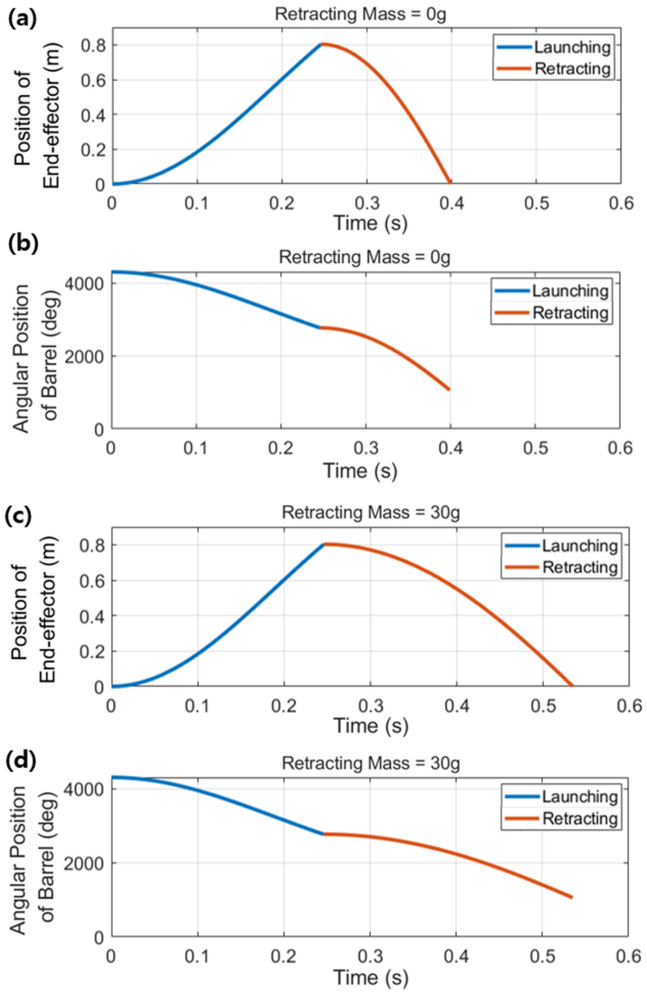

Fig. 10. Simulated data when r_b is 10.8 mm, $r_{\text{fg, forward}}$ is 7.2 mm, $r_{\text{f, forward}}$ is 20 mm, $r_{\text{fg, backward}}$ is 7.2 mm, and $r_{\text{f, backward}}$ is 18 mm. Position of (a) the end-effector and (b) the barrel gear when the retracting mass is 0 g. (c) and (d) are the positions when the retracting mass is 30 g.

launches with the initial velocity of 0 m/s and gets faster until the end-effector reaches to the 0.8 m target. When the end-effector starts to come back, it also retracts with the initial velocity of 0 m/s and the velocity gets accelerated. In terms of manipulation time, the Snatcher finishes the 0.8 m manipulation in 399 ms. The end-effector reaches the target in 246 ms and comes back in 153 ms. Retraction time is set to be shorter, considering that a target's mass may be added in a retracting phase.

Fig. 10(b) indicates the angular position of the feeder depending on the time. The feeder also gets accelerated from the initial velocity of 0 rad/s. To reach the target, the feeder rotates 1533 degrees (4.26 revolutions) within 246 ms. When the feeder retracts the end-effector, the feeder rotates 1705 degrees (4.74 revolutions) in reverse direction within 153 ms.

Fig. 10(c) and (d) indicate the position of the end-effector and the angular position of the barrel gear when the Snatcher brings a 30 g mass. When the Snatcher retracts the 30 g mass 0.8 m away, the retraction times increase from 153 ms to 289 ms as shown in Fig. 10(c). In Fig. 10(d), the amount of the angular displacement maintains but the angular speed reduces by 53% compared to when there is no retracting mass.

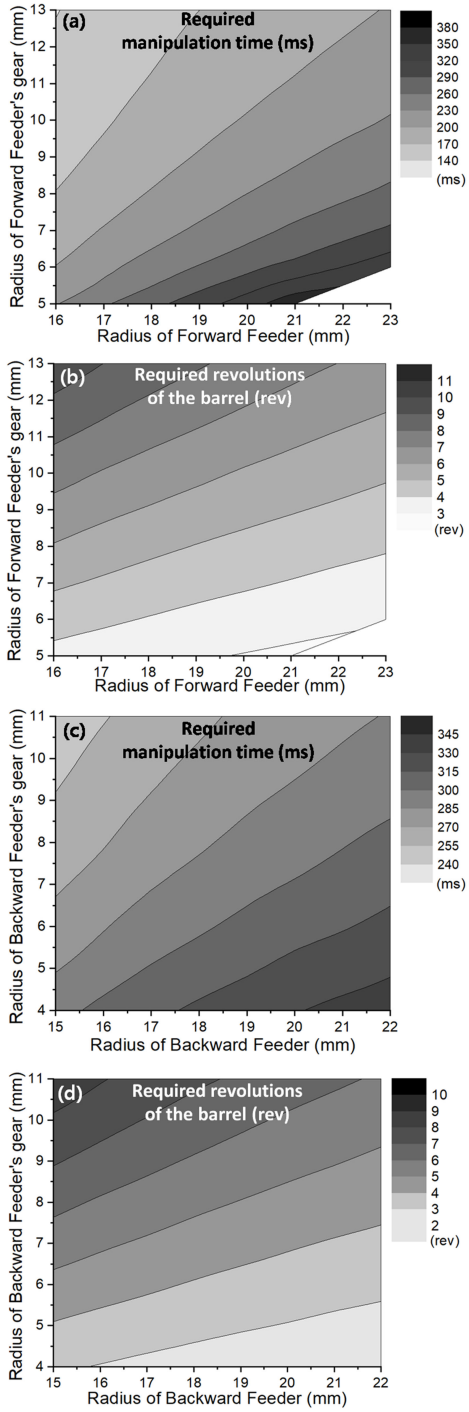

Fig. 11. The parametric study by varying the radii of the feeder's gear and the feeder. (a) The required time and (b) the required revolutions to reach 0.8 m target. (c) and (d) are when retracting the 30 g mass at a distance of 0.8 m.

B. Gear Size Selection Based on Modeling

Depending on the radii of the gears and the feeder, the Snatcher performs quite differently in terms of the required manipulation time and the required revolutions.

To investigate the effect of the parameters, Fig. 11 is given based on the modeling. Fig. 11(a) and (b) indicate the 0.8 m manipulation time and the required revolutions of the barrel, respectively. To begin with, the radius of the barrel gear is

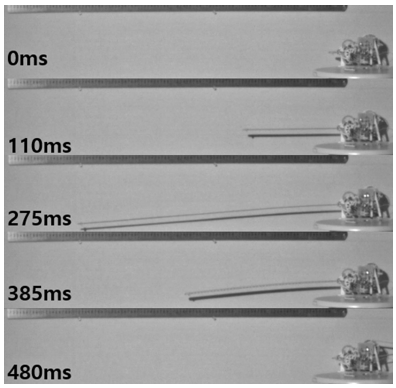

Fig. 12. Snapshots of 0.8 m snatching process.

fixed as 10.8 mm, considering the size of the wind-up spring. In Fig. 11(a), the required launching time takes longer as the radius of the forward feeder increases, and the feeder's gear radius decreases. Fig. 11(b) shows the required revolutions of the barrel to reach the target 0.8 m away. As the radius of the forward feeder increases and the feeder's gear radius decreases, the barrel needs to rotate more to reach the target.

Fig. 11(c) and (d) are when the Snatcher retracts the 30 g mass 0.8 m away. In Fig. 11(c), the required retracting time takes longer as the radius of the backward feeder increases, and the feeder's gear radius decreases. Fig. 11(d) shows the required revolutions of the barrel to retract the mass 0.8 m away. As the radius of the backward feeder increases and the feeder's gear radius decreases, the barrel needs to rotate more to reach the target

Based on the parametric study, r_{fg} and r_f are determined to fulfill the following conditions. First, the Snatcher should be able to implement at least one round trip of 0.8 m manipulation. That is, one round trip of 0.8 m manipulation should finish within 12 revolutios, which is the angular displacement output of the fully charged barrel. Second, the 0.8 m manipulation needs to finish within 600 ms for the fast snatching motion, which is determined by reference to the actual chameleon's performance [27]. To satisfy these conditions, $r_{\text{fg, forward}}$, $r_{\text{f, forward}}$, $r_{\text{fg, backward}}$ and $r_{\text{f, backward}}$ are determined as 7.2 mm, 20 mm, 7.2 mm, 18 mm, respectively.

C. Operation Test

Operation tests are done to investigate whether the Snatcher operates properly as we designed and simulated. The experiments are implemented by varying the target distance and the snatching mass. Two target distances such as 0.4 m and 0.8 m have been chosen. The target object is positioned at the chosen distances and the distance is given to the MCU through the distance sensor. Based on the distance information, the Snatcher works according to the control logic shown in Fig. 6.

To precisely analyze the manipulation process, the high-speed camera has been employed and the images have been taken with the frame rate of 1000. The images are analyzed using Kinovea. Fig. 12 shows snapshots of 0.8 m snatching process.

Fig. 13 shows both the experimental data and the simulated data for the end-effector position depending on the time. Overall,

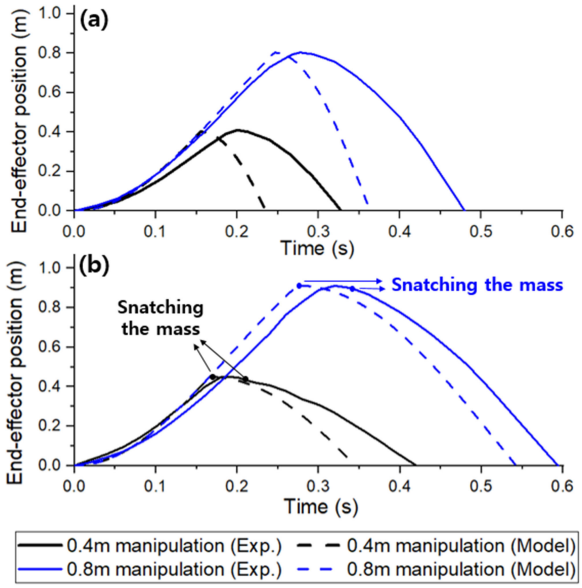

Fig. 13. Performance test. (a) Snatching manipulation without a target mass. (b) Snatching manipulation of 30 g mass.

the experimental case requires a longer time to finish the manipulation. To precisely analyze the result, the shooting process and the retracting process are separately investigated. In the case of the shooting phase, all experimental curves seem to have gradual slopes compared to the simulation although there is a difference to some extent. A similar phenomenon is shown in the retracting phase. All curves indicate a gradual decrease in the position when it comes to experimental cases.

There are some possible reasons for the difference between the simulated results and the experimental results. The first reason could be the slippage between the tapeline and the feeders. The feeders transmit the force to the tapeline through the friction. If enough friction is not given, then the tapeline does not properly work. To prevent the slip, the polymer straps are installed to the circumferences of the feeders. In the high acceleration phase such as the starting phase and the transition phase, however, the slip may occur and affect the operation.

The second is estimated to the delay during the clutching process. The clutching time is analyzed through images from the high-speed camera. It takes about 50 ms to move the SEA from the shooting feeder to the retracting feeder. That is, the start of the retraction can be delayed as much as the clutching time takes. This problem could be improved by employing high performance clutching motors or adding displacement amplifying linkages.

D. Discussion

The proposed manipulator has a limitation on the retractable mass. Fig. 14 shows the relation between the mass retracted and the required retraction time, which is calculated based on the modeling. As the mass increases, the required retraction time almost linearly increases. When the manipulator brings a 1 kg mass, for example, it takes 1.42 s to retract.

To check the objective level of the proposed manipulator, performances, working principles, and portability issues of existing

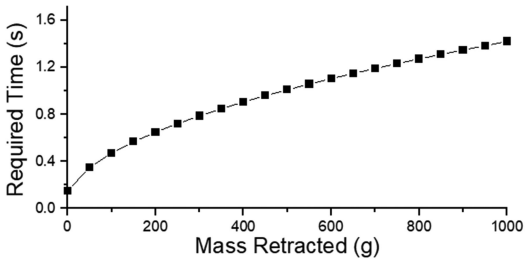

Fig. 14. Relation between the mass retracted and the required time when the manipulator brings the mass 0.8 m away.

devices are investigated in Table I. To begin with, the impact force is essential to achieve fast snatching motion. Most of existing devices employ the air compressor or the power supply to generate the high impact force, which tends to increase the system weight and deteriorate the portability. On the other hand, the proposed device weighs only 117.48 g by employing novel actuation system.

In terms of the shooting distance and the retractable mass, the Snatcher shows competitive performance by bringing 30 g mass located at 0.8 m away. Manipulation time, however, takes a bit longer while existing manipulators bring an object within 300 ms. The manipulation time would be improved in the future by employing an elastic component having high energy density.

E. Application to Mobile Systems

The Snatcher has been applied to two applications to show the possibility of use in real-world: Fast snatching manipulation for a UAV and distant manipulation for the disabled. In the attached video, the disabled use the snatcher to push the button for the elevator. In addition, the UAV tries snatching manipulation to reach a target. Likewise, we believe that the Snatcher would suggest a novel concept of mobile manipulation in the future.

V. Conclusion

Chameleons are able to catch insect prey positioned over 1.5 body lengths away. Not only do chameleons manipulate long distances, but their launching speed also is over 3.5 m/s and the acceleration reaches to over 500 m/s^2. Thanks to the surprising fast speed, chameleons bring insect prey back within a second.

Inspired by the chameleons' tongue, in this letter, we have developed a highly mobile chameleon-inspired shooting and rapidly retracting manipulator. Key design strategies are the employment of a wind-up spring and an active clutch. By applying these components, the chameleon-inspired manipulator, the Snatcher, is successfully made.

In terms of portability, which is main objective of this work, the Snatcher weighs only 117.48 g and has a size of $120 \times 85 \times 85$ mm. In addition, the Snatcher is able to bring a 30 g mass located at 0.8 m away within 600 ms. We believe the proposed device has potential to be used for fast grasping task with lightweight UAVs.

References

[1] J. H. de Groot and J. L. van Leeuwen, "Evidence for an elastic projection mechanism in the chameleon tongue," *Proc. Roy. Soc. Lond. Seri. B: Biol. Sci.*, vol. 271, no. 1540, pp. 761–770, 2004.

[2] U. K. Müller and S. Kranenbarg, "Power at the tip of the tongue," *Scie.*, vol. 304, no. 5668, pp. 217–219, 2004.

[3] D. E. Moulton, T. Lessinnes, S. O'Keeffe, L. Dorfmann, and A. Goriely, "The elastic secrets of the chameleon tongue," *Proc. Roy. Soc. A: Math. Phys. Eng. Sci.*, vol. 472, no. 2188, 2016, Art. no. 20160030.

[4] S.-J. Kim, D.-Y. Lee, G.-P. Jung, and K.-J. Cho, "An origami-inspired, self-locking robotic arm that can be folded flat," *Sci. Robot.*, vol. 3, no. 16, 2018, Paper. eaar2915.

[5] S. Kim, S. Choi, and H. J. Kim, "Aerial manipulation using a quadrotor with a two dof robotic arm," in *Proc. IEEE/RSJ Int. Conf. Intell. Robots Syst.*, 2013, pp. 4990–4995, IEEE.

[6] M. Fanni and A. Khalifa, "A new 6-DOF quadrotor manipulation system: Design, kinematics, dynamics, and control," *IEEE/ASME Trans. Mechatronics*, vol. 22, no. 3, pp. 1315–1326, Jun. 2017.

[7] T. W. Danko, K. P. Chaney, and P. Y. Oh, "A parallel manipulator for mobile manipulating UAVs," in *Proc. IEEE Int. Conf. Technol. Practical Robot Appl. (TePRA)*, 2015, pp. 1–6.

[8] A. Debray, "Manipulators inspired by the tongue of the chameleon," *Bioinspiration Biomimetics*, vol. 6, no. 2, 2011, Art. no. 026002.

[9] T. Hatakeyama and H. Mochiyama, "Shooting manipulation inspired by chameleon," *IEEE/ASME Trans. Mechatronics*, vol. 18, no. 2, pp. 527–535, Apr. 2013.

[10] T. Hatakeyama and H. Mochiyama, "Shooting manipulation system with high reaching accuracy," in *Proc. IEEE/RSJ Int. Conf. Intell. Robots Syst.*, 2011, pp. 4652–4657, IEEE.

[11] H. Mochiyama, H. Nakajima, and T. Hatakeyama, "Chameleon-like shooting manipulator for accurate 10-meter reaching," in *Proc. 10th Asian Control Conf.*, 2015, pp. 1–7.

[12] M. Kaneko, M. Higashimori, R. Takenaka, A. Namiki, and M. Ishikawa, "The 100G capturing robot-too fast to see," *IEEE/ASME Trans. Mechatronics*, vol. 8, no. 1, pp. 37–44, Mar. 2003.

[13] F. Li *et al.*, "Jumping like an insect: Design and dynamic optimization of a jumping mini robot based on bio-mimetic inspiration," *Mechatronics*, vol. 22, no. 2, pp. 167–176, 2012.

[14] M. Kovac, M. Fuchs, A. Guignard, J. C. Zufferey, and D. Floreano, "A miniature 7 g jumping robot," in *Proc. IEEE Int. Conf. Robot. Autom.*, 2008, pp. 373–378.

[15] J. Zhao *et al.*, "MSU Jumper: A single-motor-actuated miniature steerable jumping robot," *Robot. IEEE Trans.*, vol. 29, no. 3, pp. 602–614, Jun. 2013.

[16] V. Zaitsev, O. Gvirsman, U. Ben Hanan, A. Weiss, A. Ayali, and G. Kosa, "A locust-inspired miniature jumping robot," *Bioinspir Biomim.*, vol. 10, no. 6, Nov. 25 2015, Art. no. 066012.

[17] G.-P. Jung *et al.*, "JumpRoACH: A trajectory-adjustable integrated jumping-crawling robot," *IEEE/ASME Trans. Mechatronics*, vol. 24, no. 3, pp. 947–958, Jun. 2019.

[18] M. A. Woodward and M. Sitti, "MultiMo-Bat: A biologically inspired integrated jumping-gliding robot," *Int. J. Robot. Res.*, vol. 33, no. 12, pp. 1511–1529, 2014.

[19] Q.-V. Nguyen and H. C. Park, "Design and demonstration of a locust-like jumping mechanism for small-scale robots," *J. Bionic Eng.*, vol. 9, no. 3, pp. 271–281, 2012.

[20] B. G. A. Lambrecht, A. D. Horchler, and R. D. Quinn, "A small, insect-inspired robot that runs and jumps," in *Proc. IEEE Int. Conf. Robot. Autom.*, 2005, pp. 1240–1245.

[21] G.-P. Jung, C. S. Casarez, S.-P. Jung, R. S. Fearing, and K.-J. Cho, "An integrated jumping-crawling robot using height-adjustable jumping module," in *Proc. IEEE Int. Conf. Robot. Autom.*, 2016, pp. 4680–4685.

[22] D. W. Haldane, M. M. Plecnik, J. K. Yim, and R. S. Fearing, "Robotic vertical jumping agility via series-elastic power modulation," *Sci. Robot.*, vol. 1, no. 1, pp. 1–9, 2016.

[23] L. Bai, F. Zheng, X. Chen, Y. Sun, and J. Hou, "Design and experimental evaluation of a single-actuator continuous hopping robot using the geared symmetric multi-bar mechanism," *Appl. Sci.*, vol. 9, no. 1, pp. 1–24, 2019.

[24] K. Schwenk and D. Bell, "A cryptic intermediate in the evolution of chameleon tongue projection," *Experientia*, vol. 44, no. 8, pp. 697–700, 1988.

[25] L. J. Vitt, E. R. Pianka, J. Cooper, E. William, and K. Schwenk, "History and the global ecology of squamate reptiles," *Amer. Naturalist*, vol. 162, no. 1, pp. 44–60, 2003.

[26] A. Herrel, J. J. Meyers, P. Aerts, and K. C. Nishikawa, "Functional implications of supercontracting muscle in the Chameleon tongue retractors," *J. Exp. Biol.*, vol. 204, no. 21, pp. 3621–3627, 2001.

[27] P. C. Wainwrigth, D. M. Kraklau, and A. F. Bennett, "Kinematics of tongue projection in Chamaeleo oustaleti," *J. Experi. Biol.*, vol. 159, no. 1, pp. 109–133, 1991.